Seasonality of volcanic eruptions

B. G. Mason and D. M. Pyle
Department of Earth Sciences, Cambridge University, Cambridge, UK

W. B. Dade[1]
Institute of Theoretical Geophysics, Cambridge University, Cambridge, UK

T. Jupp[2]
BP Institute for Multiphase Flow, Cambridge University, Cambridge, UK

Received 5 November 2002; revised 10 March 2004; accepted 16 March 2004; published 27 April 2004.

[1] An analysis of volcanic activity during the last three hundred years reveals that volcanic eruptions exhibit seasonality to a statistically significant degree. This remarkable pattern is observed primarily along the Pacific "Ring of Fire" and locally at some individual volcanoes. Globally, seasonal fluctuations amount to 18% of the historical average monthly eruption rate. In some regions, seasonal fluctuations amount to as much as 50% of the average eruption rate. Seasonality principally reflects the temporal distribution of the smaller, dated eruptions (volcanic explosivity index of 0–2) that dominate the eruption catalog. We suggest that the pattern of seasonality correlates with the annual Earth surface deformation that accompanies the movement of surface water mass during the annual hydrological cycle and illustrate this with respect to global models of surface deformation and regional measurements of annual sea level change. For example, seasonal peaks in the eruption rate of volcanoes in Central America, the Alaskan Peninsula, and Kamchatka coincide with periods of falling regional sea level. In Melanesia, in contrast, peak numbers of volcanic eruptions occur during months of maximal regional sea level and falling regional atmospheric pressure. We suggest that the well-documented slow deformation of Earth's surface that accompanies the annual movements of water mass from oceans to continents acts to impose a fluctuating boundary condition on volcanoes, such that volcanic eruptions tend to be concentrated during periods of local or regional surface change rather than simply being distributed randomly throughout the year. Our findings have important ramifications for volcanic risk assessment and volcanoclimate feedback mechanisms. *INDEX TERMS:* 5480 Planetology: Solid Surface Planets: Volcanism (8450); 5499 Planetology: Solid Surface Planets: General or miscellaneous; 7299 Seismology: General or miscellaneous; *KEYWORDS:* periodicity volcano, Earth's shape, mass redistribution

Citation: Mason, B. G., D. M. Pyle, W. B. Dade, and T. Jupp (2004), Seasonality of volcanic eruptions, *J. Geophys. Res.*, *109*, B04206, doi:10.1029/2002JB002293.

1. Introduction

[2] Volcanism is a key process role at Earth's surface, with tens of new eruptions starting every year. Despite the environmental significance of volcanic eruptions, the factors that influence the onset of eruptions remain poorly understood. One hypothesis that has been proposed is that seasonal changes in the eruption rate of volcanoes may result from annual fluctuations in crustal load associated with changes in sea level, or atmospheric pressure, driven by the hydrologic cycle [*McNutt and Beavan*, 1987; *Neuberg*, 2000]. Such a pattern has been proposed for the volcano Pavlof on the Alaskan Peninsula, North America [*McNutt*, 1999].

[3] If correct, such links between climate and tectonics would not only contribute to an improved understanding of volcanic hazards, but would also provide support for ideas regarding enhanced volcanic activity during periods of global sea level change in the geologic past. Increased rates of volcanism have been correlated with, for example, the onset of glaciations and attendant rapid drops in sea level [*Rampino et al.*, 1979], deglaciation and ice removal from Iceland [*Jull and McKenzie*, 1996] and eastern California [*Glazner et al.*, 1999], and rates of sea level change in the Mediterranean [*McGuire et al.*, 1997]. The modulation of

[1]Now at Department of Earth Sciences, Dartmouth College, Hanover, New Hampshire, USA.
[2]Now at Centre for Ecology and Hydrology, Natural Environment Research Council, Monks Wood, Huntingdon, UK.

0148-0227/04/2002JB002293$09.00

volcanic activity on seasonal timescales in the modern era would indicate that ongoing processes may serve as a real-time analogue for phenomena previously assumed to occur only over geologic time. Seasonal patterns in eruption rate would also suggest that observed correlations between seismic or eruptive activity and meteorological parameters on local scales (e.g., storms at Mount St Helens [*Mastin*, 1994], pressure fluctuations at Stromboli, Italy [*Neuberg*, 2000], or rainfall events on Montserrat, West Indies [*Matthews et al.*, 2002]) are but components of a larger-scale relationship between volcanic activity and global climate.

[4] With these ideas in mind, we analyzed the Smithsonian catalogue of volcanic eruptions [*Simkin and Siebert*, 1994] for temporal patterns in eruption rates on global and regional scales. The Smithsonian catalogue includes the start dates of more than 3200 subaerial eruptions and eruption sequences recorded during the last 300 years. It is the most comprehensive compilation of worldwide volcanic activity currently available.

[5] A review of earlier studies of temporal patterns of eruption rates is given by *McNutt* [1999]. We simply note here that earlier analyses were based on older, incomplete data or relied on observations of very small numbers of events at only one or two volcanoes. As a result, the significance of temporal patterns of eruption rates (or their absence) proposed in the literature has remained in question [e.g., *Hamilton*, 1973; *Stothers*, 1989]. In considering the Smithsonian catalogue here, we adopt a global perspective using eruptions of all sizes. This perspective distinguishes our study from previous efforts. In Figure 1 we present the data on which our subsequent analysis is based. As Figure 1a shows, there is a clear variation in the monthly start rate of eruptions from the past 300 years, which persists whether we use a coarser data set (using all eruptions where at least the start month is known), or our preferred data set, using eruptions with a precisely known start date. A clear seasonal pattern is evident, with more eruptions reported as starting between November and April, than between April and October. This global pattern of volcanic seasonality has not been recognized previously, principally because earlier analyses of similar data were focused primarily on the "large" eruptions [e.g., *Stothers*, 1989]. As Figure 1b shows, smaller or nonexplosive eruptions (with a volcanic explosivity index of 0–2) dominate the data set: most of the eruptions whose start dates define the seasonal volcanic pattern are small explosive events. We return to the full statistical treatment of this pattern, and its implications, in the next section.

[6] Among the global-scale mechanisms once considered likely to trigger volcanic eruptions are the diurnal and fortnightly tidal forces in the Earth's crust [*Mauk and Johnston*, 1973; *Dzurisin*, 1980; *Emter*, 1997]. To assess the potential effects of such forces, we initially analyzed the dates of volcanic eruptions recorded by *Simkin and Siebert* [1994] with respect to the lunar phase of historical tides [*Wenzel and Hartmann*, 1994] using the statistical methods described below. We found no conclusive evidence for a general correlation between volcanic activity and lunar tidal phase. This result is consistent with recent work which indicates that diurnal and fortnightly tidal stresses may be too short-lived and strain rates too high to effect a significant viscous response in partially molten regions of the Earth's subsurface [*Rydelek et al.*, 1992; *Neuberg*, 2000].

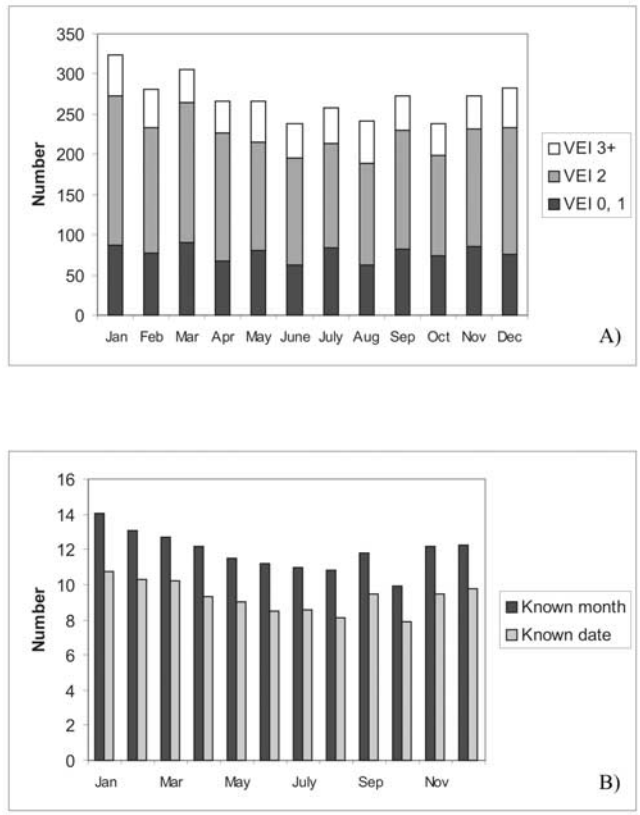

Figure 1. Histograms of raw data from the Smithsonian eruption catalogue, plotted to show the nature of the volcanic eruption data on which the analysis is based. (a) Monthly pattern of eruption rates for 1700 AD to 1999 AD, for eruptions with known start dates (month and day); and for eruptions with known start months. (b) Histogram of eruption rates for eruptions with known start dates, grouped by eruption size (volcanic explosivity index (VEI) [*Newhall and Self*, 1982]). Eruptions of VEI 2 (smaller explosive eruptions) dominate the data set.

[7] We tentatively relate the findings of our analysis instead to annual harmonics of crustal motion as assessed by *Mangiarotti et al.* [2001], which are associated primarily with seasonal changes in snowpack thickness and soil moisture [e.g., *van Dam et al.*, 1997]. This is one of a number of recent publications that describe the global-scale crustal displacements that are associated with the annual interhemispheric movements of water mass ($\sim 10^{16}$ kg [*Blewitt et al.*, 2001]), and ocean-continent water mass exchange ($\sim 3 \times 10^{15}$ kg [*Blewitt and Clarke*, 2003]). These displacements may have amplitudes of order 10 mm, and have been detected both in satellite laser ranging data [e.g., *Cheng and Tapley*, 1999; *Bouillé et al.*, 2000; *Mangiarotti et al.*, 2001] and by inversion of terrestrial GPS data [e.g., *van Dam et al.*, 2001; *Wu et al.*, 2003; *Blewitt and Clarke*, 2003]. At the present time, these inversions and models are still converging, but they produce grossly consistent first-order results. The general pattern [*Blewitt et al.*, 2001] is that over the course of a year, the Northern Hemisphere firstly compresses (peaking in February and March), and

Table 1. Raw Eruption Rate Data for All Regions Described in Text[a]

Observations	January	February	March	April	May	June	July	August	September	October	November	December
Global												
1700–1999	325	328	295	297	261	264	253	250	288	242	302	275
1700–1899	102	106	87	85	79	83	66	89	95	74	88	92
1900–1999	223	222	208	212	182	181	187	161	193	168	214	183
Regional, 1700–1999												
South America	30	29	14	18	13	12	17	17	16	21	18	21
Central America	21	23	26	12	20	10	11	13	24	22	16	20
Alaskan Peninsular	1	2	10	3	3	7	10	6	6	1	6	1
Kamchatka	13	14	18	15	11	12	10	7	11	9	7	10
Kyushu and Ryuku	15	18	9	22	9	9	9	5	16	8	17	13
Melanesia	14	8	11	11	11	7	5	5	6	11	13	10
Kurile Islands	5	8	3	7	5	6	8	4	5	5	8	3
Honshu and Hokkaido	24	24	19	26	20	23	28	24	21	16	25	16
Philippines	9	8	6	4	6	9	10	5	11	9	7	7
Indonesia	60	68	62	69	73	59	47	68	60	49	67	54
Mediterranean	20	18	16	15	10	18	19	21	14	15	22	17
Iceland	8	4	4	7	7	6	4	8	7	7	4	6
Hawaii	13	13	7	8	9	5	7	12	9	2	12	8
Reunion	9	14	10	7	8	12	10	8	7	3	13	13
Individual volcanoes												
Sakura-jima, Japan (1956–1997)	683	544	596	495	533	598	481	533	624	620	651	771
Semeru, Indonesia[b] (1997–2000)	85	77	73	77	73	76	65	79	85	95	88	94

[a]Columns indicate the numbers of eruptions known to have started within each "month" (1/12 of a year), globally and regionally. Data are from *Simkin and Siebert* [1994].

[b]The Semeru data are reported as mean eruptions per day in each given "month," based on the days for which data are available.

then expands (August, September), while the Southern Hemisphere behaves conversely, while the ocean mass reaches a maximum in late August. In our analysis, we have chosen to compare our results with the model of *Mangiarotti et al.* [2001] simply because this was the model most readily available at the time that we completed this work. The resolution of these models is still, however, very coarse. For example, the existence of tectonic plates, and plate boundaries, cannot be seen in the models – even though plate boundaries may have a substantial influence on local deformation patterns (for example, at subduction zones where a continental plate is juxtaposed against an oceanic plate). For this reason, we do not attempt to draw anything other than general conclusions from the pattern of Earth surface deformation.

[8] To show the regional patterns, we illustrate the potential significance of seasonal fluctuations in sea level as assessed remotely with geodetic data by *Minster et al.* [1999], directly using coastal tide gauge data by *Tsimplis and Woodworth* [1994], and fluctuations in regional atmospheric pressure as reported by *Landsberg* [1984].

[9] Motivated by the results of our analysis of the catalogue data, we undertook independent tests of seasonality in two additional time series. These records are of small, ongoing, open-vent eruptions which include (1) more than 7100 instrumentally recorded events during the period 1956–1997 at volcano Sakura-jima, Japan (K. Ishihara, personal communication, 2001) and (2) more than 96,000 explosive events, recognized on local seismographs, during the period 1997–2000 at volcano Semeru, Indonesia (Volcanological Survey of Indonesia, personal communication, 2001). These events are each distinct explosions ("Vulcanian" explosions) that are generally thought to originate at shallow levels in a volcanic conduit.

[10] Since these time series represent smaller-scale, higher-frequency (hourly to daily), phenomena than the discrete eruptions that are typically recorded by *Simkin and Siebert* [1994], their consideration provides an important complement to the perspectives, which emerge from the analysis of the larger catalogue. It is possible, however, that there may be fundamental differences between the factors that influence the onset of a discrete eruption at a previously quiet volcano, and those that influence the onset of one explosion that is part of a persistent sequence of activity.

[11] The methods used to delineate seasonality in eruption rates and environmental forcing, are described in the following section. We then present the results of an analysis of the data described above using these methods, and discuss key findings.

2. Methods

2.1. Statistical Analysis

[12] Recorded observations of the start date of single eruptions and significant eruption sequences reported by *Simkin and Siebert* [1994] were grouped according to time of year for (1) phenomena observed worldwide during the overlapping periods 1700–2000, 1700–1899, and 1900–2000; and (2) phenomena observed during the period 1700–2000 in the major geographic regions identified by Simkin and Siebert for which the average total number of eruptions in a month equaled or exceeded 5. This threshold number represents a conservative criterion for the applicability of the statistical tests employed in our analysis and described below [*Conover*, 1980]. The observed start dates were then grouped into twelve bins, each corresponding to exactly 1/12 part of the year, which correspond approximately with the months of the year. The correspondence is not exact because of the varying number of days in each month but for simplicity we use the names of the months as labels for the bins. We summarize the full set of data on which our analysis was based in Table 1.

[13] In our analysis we have not employed any filters to the Smithsonian data set, other than to focus on eruptions

Table 2. Sea Level Cycles Calculated From Satellite Altimetry and Coastal Tide Gauge Data[a]

			Annual		Semiannual	
Region/Station	Longitude	Latitude	Amplitude	Phase	Amplitude	Phase
Global			9.5	−3.5		
SW South America						
Tumaco (25)	78°44′W	01°50′N	41.02	−4.01	36.79	−0.86
La Libertad (31)	80°54′W	02°12′S	18.11	2.29	11.59	−0.91
Antofagasta (39)	70°24′W	23°39′S	36.20	2.31	13.21	0.25
Talcahuano (33)	73°06′W	36°41′S	40.03	4.60	29.96	0.22
West Central America						
Acapulco (33)	99°54′W	16°50′N	76.01	−4.01	28.58	0.52
Acajutla (24)	89°50′W	13°34′N	50.81	−4.11	17.53	−0.39
Quepos (32)	84°09′W	09°24′N	38.02	−3.56	34.53	−0.47
Alaskan Peninsula						
Unalaska (21)	166°32′W	53°53′N	71.14	−0.49	22.96	0.08
Kodiak (19)	152°31′W	57°43′N	80.79	−0.92	7.44	−1.45
Kamchatka (34)	158°39′E	52°59′N	86.91	0.42	40.30	0.61
Sakura-jima, Japan						
Hoso-jima (90)	131°40′E	32°26′N	139.40	−4.28	15.02	2.80
Aburatsu (31)	131°25′E	31°34′N	138.15	−4.15	17.57	2.67
Semeru, Indonesia						
Pacitan (4)	111°05′E	08°12′S	82.82	1.65	43.85	−1.44
Surabaya (7)	112°36′E	07°12′S	64.19	−1.70	32.52	1.78
Semarang (7)	110°24′E	07°00′S	35.76	5.27	35.34	−1.22
Melanesia (13)	152°11′E	4°12′S	44.48	1.85	20.10	−2.33

[a]Amplitudes are given in millimeters. Phase indicates date of maximal sea level in months from start of year. Number in parentheses after regional stations indicates number of years in tide gauge record. Functional descriptions of global and regional sea level patterns taken from *Minster et al.* [1999] and *Tsimplis and Woodworth* [1994], respectively.

with known start dates. It is also worth noting that our analysis focuses on the starting point of eruptions, and not on the main, or climactic, phase of the event. In some cases there may be periods of weeks or months between the start date of an eruption, and the main eruptive event [*Simkin and Siebert*, 1994]. Furthermore, we have made no corrections to the data to allow for the changing rate of reporting of eruptions over the past 300 years. As we show below, we see the same statistically significant pattern of seasonality in data from 18th, 19th and 20th centuries; this gives us confidence that low reporting rates of smaller eruptions early in the catalogue do not lead to any detectable inbuilt seasonal bias (for example, due to possible underreporting of tropical eruptions during local wet seasons). Finally, the catalogue on which the analysis is based is principally a record of visually observed eruptions. Volcanospecific instrumental catalogues of eruptions (for example of events detected by seismicity) provide an independent test of the seasonal patterns of the main catalogue. For this reason, we examined two long instrumental eruption records, for eruptions of Sakura-jima (Japan) and Semeru (Java, Indonesia). For these examples, we assessed the number of small explosions detected by local seismic stations that occurred in each month during the period 1956–1997 and 1997–2000, respectively.

[14] For each data set, two tests were undertaken of a null hypothesis of uniform eruption frequency. The first was a test for general nonuniformity based on the Chi-square statistic Y defined in terms of expected monthly number of eruptions m and the observed number n for each of $k = 12$ "months". The Chi-square statistic is given by

$$Y = m \sum_{i=1}^{k} E_i^2, \tag{1}$$

where $E_i \equiv (n_i - m)/m$, the expected monthly average $m \equiv N/k$, and the total number of eruptions N is given by

$$N = \sum_{i=1}^{k} n_i. \tag{2}$$

Significant deviations from uniform occurrence are associated with Y values that exceed critical values for $k - 1$ degrees of freedom. Critical values and relevant levels of confidence α are given by *Fisher* [1993].

[15] The second test was a Rayleigh test based on the mean resultant length R given by

$$R^2 = C^2 + S^2, \tag{3}$$

Table 3. Predicted Annual Harmonics of Crustal Motion Associated With Observed Changes in Soil Moisture and/or Snowpack[a]

			Annual	
Location	Longitude	Latitude	Amplitude	Phase
Andes	76°15′W	8°45′S	1.4	−2.8
Andes	73°45′W	11°15′S	1.3	−3.1
Andes	66°15′W	18°45′S	3.0	−2.9
Andes	66°15′W	23°45′S	2.3	−2.7
Andes	68°45′W	28°45′S	0.9	−2.7
Central America	91°15′W	13°45′N	2.4	3.2
Alaskan Peninsula	162°45′W	56°15′N	0.2	−1.4
Kamchatka	158°45′E	56°15′N	0.7	−4.4
Kyushu	128°45′E	31°15′N	0.5	1.7
Java, Indonesia	111°15′E	8°45′S	0.3	−3.4
Melanesia	158°45′E	8°45′S	0.7	9.5

[a]Amplitudes are given in millimeters. Phase indicates date of maximal crustal elevation in months from start of year. Regional harmonic coefficients provided by S. Mangiarotti and are derived from the model described by *Mangiarotti et al.* [2001].

Table 4. Annual and Semiannual Harmonics of Global and Regional Atmospheric Pressure[a]

Region	Longitude	Latitude	Annual		Semiannual	
			Amplitude	Phase	Amplitude	Phase
Global			0.6	−4.5		
SW South America						
Antofagasta	70°24′W	23°39′S	22.3	−4.9	8.6	3.4
Santiago	70°42′W	33°27′S	21.2	−5.1	2.3	3.3
Concepción	73°03′W	36°40′S	20.6	−4.4	5.9	3.2
Central America						
Acapulco	96°56′W	16°50′N	8	0.5	6.5	0.5
San Jose	84°08′W	9°56′N	10	0.1	6.2	0.45
Alaskan Peninsula	166°32′W	53°53′N	60.1	5.7	18.8	−4.6
Kamchatka	158°45′E	52°58′N	46.2	−6.4	18.4	3.4
Kyushu	129°52′E	32°44′N	7.3	0.34	0.9	4.33
Java, Indonesia						
Djakarta	106°39′E	6°10′S	5.2	−3.3	1.9	1.3
Surabaya	112°36′E	07°12′S	9.0	−3.9	3.6	1.1
Melanesia	152°11′E	04°12′S	17.1	−5.0	3.5	3.42

[a]Amplitudes are given in millibars. Phase indicates date of maximal crustal elevation in months from start of year. Global coefficients are from *Minster et al.* [1999] and pertain to average pressures over oceanic areas from NCEP/NCAR observations. Regional harmonics generated by least squares regression analysis of long-term monthly means reported by *Landsberg* [1984].

where

$$C = \frac{1}{N}\sum_{i=1}^{k} n_i \cos(\theta_i) \text{ and } S = \frac{1}{N}\sum_{i=1}^{k} n_i \sin(\theta_i), \qquad (4)$$

and θ_i represents the date at the center of each monthly bin i expressed as a radian angle in the range $\{0, 2\pi\}$. This test is well suited for detecting a single, modal direction in a sample of vectors. In this particular application, the null hypothesis of uniformity is rejected if R exceeds a critical value. The confidence level P associated with the mean resultant length R in a single Rayleigh test is given by

$$P = \exp(-Z)\left[1 + \left(2Z - Z^2\right)/4N - \left(24Z - 132Z^2 + 76Z^3 - 9Z^4\right)/288N^2\right], \qquad (5)$$

where $Z \equiv NR^2$ [*Fisher*, 1993]. For an eruption record for which $P < 0.05$, the mean month of eruption occurrence M was evaluated in terms of the record's trigonometric moment [*Fisher*, 1993], where

$$M = \begin{cases} \tan^1(S/C) & \text{if } S > 0, C > 0 \\ \tan^{-1}(S/C) + \pi & \text{if } C < 0 \\ \tan^{-1}(S/C) + 2\pi & \text{if } S < 0, C > 0 \end{cases}. \qquad (6)$$

[16] The Chi-square and Rayleigh tests are conventional statistical tools. They should be familiar to all Earth scientists who have evaluated the statistical properties of directional data pertaining to, for example, current velocities in the atmosphere and ocean, or the orientations of sedimentary bed forms or elongate grains in rocks. The Rayleigh test is a more rigorous discriminator of spatial or sequential nonuniformity than the Chi-square test, and is better suited to detect patterns that are unimodal or equivalently, in this case, clearly annual in recurrence. Since most of the data that we have examined show annual, rather

Table 5. Summary of Statistical Analysis of Seasonality of Volcanic Eruptions[a]

Observations	*N*	*m*	*Y*	α	*R*	*P*	*M*
Global							
1700–1999	3386	0.9	32.2	<0.001	0.054	<0.001	Jan.
1700–1899	1052	0.4	15.8	0.15	0.060	0.02	Jan.
1900–1999	2334	1.9	24.6	0.01	0.053	0.002	Jan.–Feb.
Regional, 1700–1999							
South America	227	0.06	19.0	0.06	0.16	0.004	Jan.
Central America	220	0.06	18.5	0.07	0.13	0.02	Jan.
Alaskan Peninsula	56	0.02	25.9	0.01	0.28	0.01	June–July
Kamchatka	137	0.04	10.1	>0.2	0.16	0.03	March
Kyushu & Ryukyu Is.	150	0.04	22.8	0.02	0.14	0.04	Jan.–Feb.
Melanesia	112	0.03	11.0	>0.2	0.17	0.04	Jan.
Individual volcanoes							
Sakura-jima, Japan (1956–1997)	7123	14.1	128.5	<0.001	0.073	<0.001	Nov.
Semeru, Indonesia (1997–2000)	96,011	2000	33.0	<0.001	0.107	<0.001	Nov.

[a]*N* indicates total number of eruptions; *m* indicates mean monthly number of eruptions; *Y* and α are the Chi-squared statistic and the related significance level of a nonuniform annual pattern in eruption rate, respectively; *R* and *P* are the Rayleigh statistic and the related significance level of a seasonal peak in eruption rate; *M* indicates modal month of eruption.

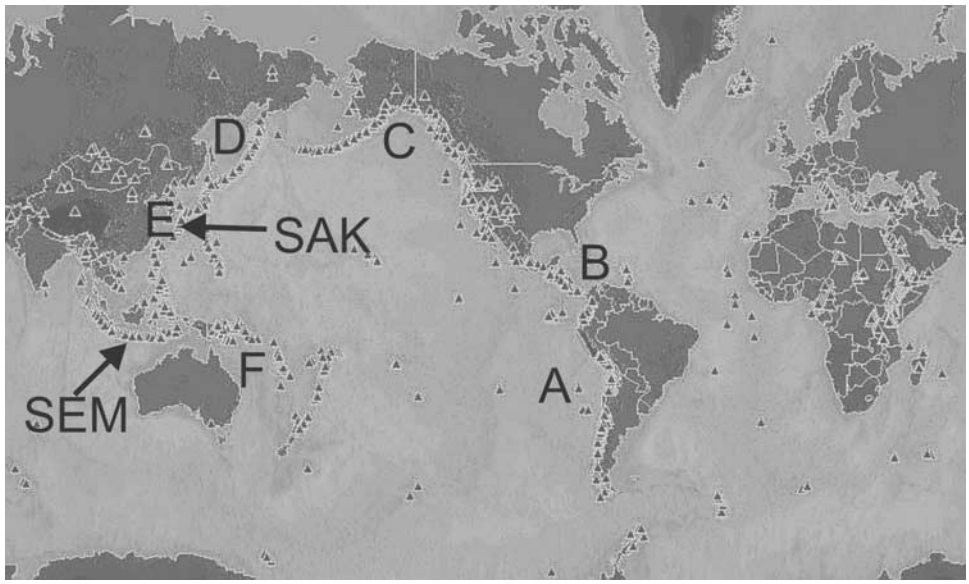

Figure 2. Global map of the locations of active volcanoes, annotated to show some of the key regions and volcanoes mentioned in the text. Small triangles show the locations of all known volcanoes, and letters denote regions and volcanoes mentioned as follows: A, South American Andes; B, Central America; C, Alaskan Peninsula; D, Kamchatka; E, Kyushu and Ryuku; F, Melanesia; SAK, Sakurajima volcano; SEM, Semeru volcano. Figure adapted from the Smithsonian Institution global volcano map at http://www.volcano.si.edu/gvp/world/location.cfm.

than semiannual, patterns of behavior, we have not used any of the other statistical tests that might be better suited to bimodal data sets; our emphasis here is simply to demonstrate that there is significance to the annual seasonal pattern of eruption start dates.

[17] The analysis of data from the Smithsonian catalogue is not confirmatory. That is, the probabilities of statistical significance emerging from our analysis of the data catalogued by *Simkin and Siebert* [1994] are nominal values uncorrected for the multiple, exploratory comparisons undertaken here. In contrast, our analyses of the time series from volcanoes Sakura-jima and Semeru represent a priori tests of the perspectives that emerged from our analysis of the Smithsonian catalogue.

2.2. Assessment of Seasonal Crustal Motion and Climatology

[18] The analysis of eruption occurrence described above was undertaken in the context of (1) annual fluctuations in sea level measured remotely on the global scale and summarized by *Minster et al.* [1999] and by tidal gauge at selected locations as reported by *Tsimplis and Woodworth* [1994], (2) inferred annual fluctuations of crustal elevation related to changes in snowpack and soil moisture as reported by *Mangiarotti et al.* [2001] (also S. Mangiarotti, personal communication, 2002), and (3) long-term average monthly values of atmospheric pressure at representative locations in each region as summarized by *Landsberg* [1984]. Global sea levels pertain to changes in total water mass in the world ocean associated with the annual hydrologic cycle, and corrected for steric changes in density. Annual and semiannual cycles in sea level measured directly at coastal tide gauges reflect changes in air pressure, steric density, and regional runoff [*Chen et al.*, 1998; *Cazenave et al.*, 1999]. The functional forms of the annual and semiannual harmonics of each of these parameters, used to calculate the curves shown in various figures introduced below, are given in Tables 2–4.

3. Results

[19] The results of our statistical analysis of the seasonal occurrence of volcanic eruptions are presented in Table 5, which includes only those subsets of the data (from Table 1) that reveal statistically significant evidence for seasonality. Levels of statistical significance for the Chi-square and Rayleigh tests are indicated by the reported vales of α and P, respectively.

[20] Seasonality of the eruptions catalogued by *Simkin and Siebert* [1994] is clearly indicated on a global scale. In terms of the Rayleigh test, the levels of significance of seasonality in eruption rates are, in general, less than 10%. That is, if eruptions do occur uniformly in time, then there is only a 10% chance of obtaining the supercritical values of the mean resultant length reported here. This finding does not depend on the century considered. Seasonality in eruption rate is also indicated regionally during the period 1700–1999 at volcanoes in the Andes, Central America, the Alaskan Peninsula, Kamchatka, on the Kyushu and Ryukyu Islands of Japan, and in Melanesia (Figure 2). Each of these arc segments comprises records of eruptions at tens of volcanoes, but with a smaller number of volcanoes contributing substantially to the data set. For example, for Kyushu-Ryuku, five volcanoes (Suwanose-Jima, Kuchinoerabu-Jima, Sakura-jima, Kirishima and Aso) dominate the data set; while in the Aleutians - Alaskan Peninsula, most of the data derive from 20th century eruptions of nine volcanoes (of which one is Pavlof).

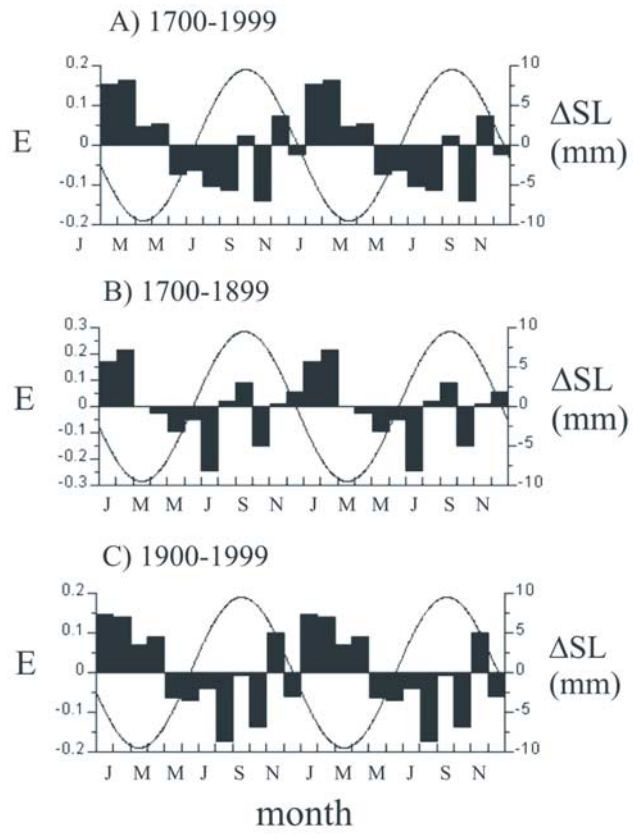

Figure 3. Monthly anomalies E_i of worldwide volcanic eruption rate during period (a) 1700–1999, (b) 1700–1899 only, and (c) 1900–1999 only. Anomalies represent the number of eruptions in a given month above or below the average monthly value m and normalized by m (see section 2). The solid lines indicate the annual cycle in global sea level observed with satellite altimetry [*Minster et al.*, 1999] (see Table 2). Note that the horizontal axes span 24 months to aid in the visualization of annual patterns.

[21] Average months of peak eruption rate for all significant seasonal patterns correspond to boreal winter months January–March, with the exception of the Alaskan peninsula where historic eruptions, at least those recorded in the Smithsonian catalogue, have preferentially occurred, on average, during boreal summer. Seasonal patterns in regional eruption rate could not be identified with confidence in the Kurile Islands, the Japanese islands of Honshu and Hokkaido, the Philippines, Indonesia, the Mediterranean, or at several oceanic islands associated with hot spot activity including, individually, Iceland, Hawaii, and Reunion (see Table 1 for the raw data).

[22] Statistically significant patterns of seasonality are observed in the sequence of nearly continuous eruptions at Sakura-jima during the period 1956–1997, and at Semeru during the period 1997–2000. At both volcanoes, the seasonal eruption rate exhibits a maximum during the month of November, although the Semeru record shows generally enhanced activity from September–January, rather than a single defined peak. An interesting feature of the activity at Sakura-jima, in common with the instrumental records from Pavlof volcano, Alaska [*McNutt*, 1999], is that the activity peaks in November recognized in the instrumental records do not coincide with the regionally averaged peak of activity shown by the relevant volcanic arc segment (Kyushu, in the case of Sakura-jima; Alaska, in the case of Pavlof). Further

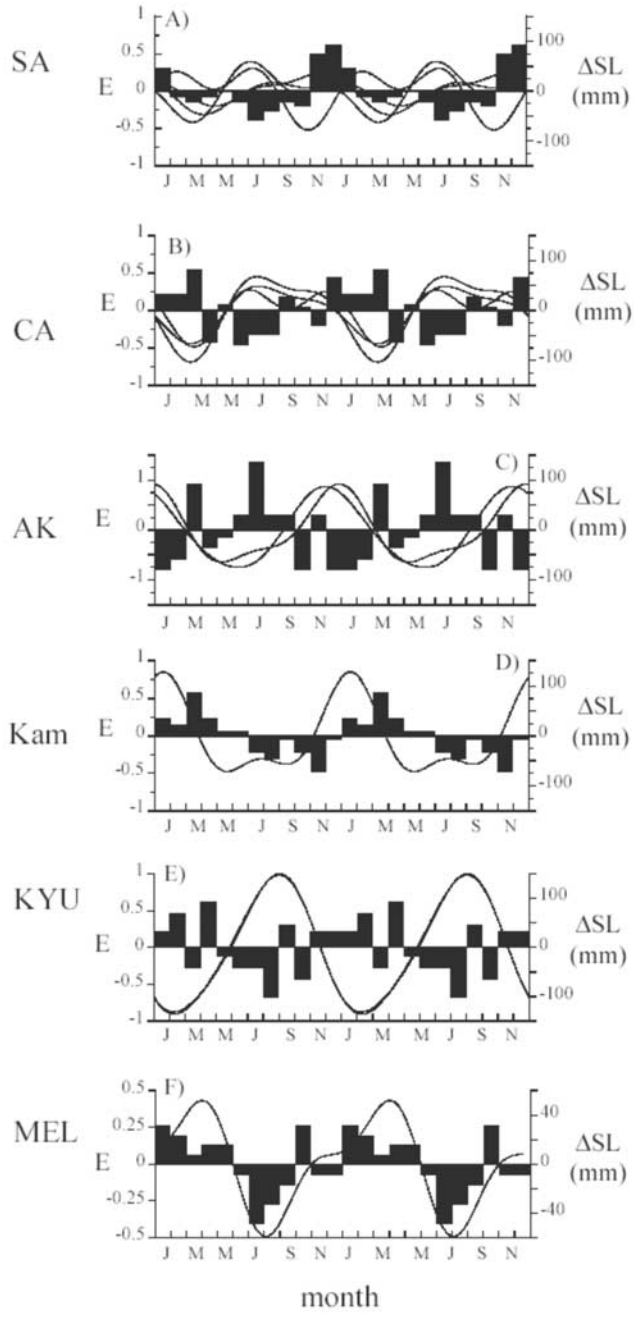

Figure 4. Monthly anomalies of volcanic eruption rate during period 1700–1999 in (a) South American Andes, (b) Central America, (c) Alaskan Peninsula, (d) Kamchatka, (e) Kyushu and Ryuku, and (f) Melanesia. The solid lines in each panel indicate the annual cycles in regional sea level recorded at coastal tide gauges as reported by *Tsimplis and Woodworth* [1994] and listed here in Table 2. Note that the horizontal axes span 24 months to aid in the visualization of annual patterns.

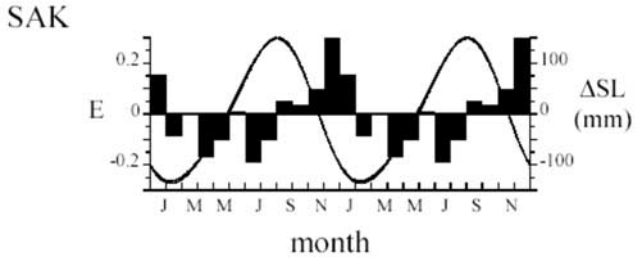

Figure 5. Monthly anomalies of volcanic eruption rate at Sakura-jima (Kyushu, Japan) during years 1956–1997. Otherwise as in Figure 2. Note that the horizontal axes span 24 months to aid in the visualization of annual patterns.

analysis of instrumental records of recently active volcanoes is needed to establish the extent to which local, regional and global patterns converge, or diverge, and to discover the extent to which individual volcanoes that are spatially close to one another show similar patterns of seasonality. One further point to note from Figure 3 is that the November-December peak of activity at Sakura-jima corresponds with the maximal rate of sea level fall. We return to this point later.

[23] Normalized monthly deviations E from the expected, long-term average monthly eruption rate for records exhibiting seasonal patterns, for which $P < 0.05$ listed in Table 5, are shown in Figures 3–6 Note that the horizontal axes of Figures 3–6 span 2 years to aid in the visualization of the proposed seasonal patterns. Annual fluctuations amount to 18% of the global monthly mean eruption rate (Figure 3), and can amount to in excess of 50% of some regional monthly mean eruption rates (Figure 4). At individual volcanoes Sakura-jima and Semeru, seasonal fluctuations amount to approximately 25–30% of the monthly mean eruption rate (Figures 5 and 6, respectively).

[24] Also shown in each of Figures 3–6 are the deviations from long-term mean sea level assessed globally using satellite altimetry [*Minster et al.*, 1999], and assessed regionally using tide gauge data from representative locations with relatively long records and as reported by *Tsimplis and Woodworth* [1994]. The annual and semiannual components of the seasonal sea level changes depicted in Figures 3–6 are summarized in Table 2. We note that, for the cases shown here and for which seasonality is observed, annual peaks in eruption rates generally occur during intervals of falling or lowest annual sea levels. Such correlations are observed whether eruptions and sea level changes are considered globally (Figure 3), regionally (Figure 4) or at an individual volcano with a substantial record (Figure 5). Exceptions to this correlative pattern include (1) the Andes of SW South America (Figure 4), (2) Melanesia, and (3) at the volcano Semeru, Indonesia (Figure 6). The lack of correlation between seasonal eruption rates and sea level in South America and at Semeru mainly reflects the absence of a regional pattern in seasonal sea level changes. In Melanesia, seasonal peaks in eruption rate coincide with an annual maximum in sea level.

[25] Shown in Figure 7 is a plot of the lag of eruption rate maximum (M, see equation (6) and Table 5) for selected regions and volcanoes preceding an annual peak in inferred elevation of regional crust (varying in response to changes in soil moisture and snowpack) or following an annual maximum in the long-term, regional atmospheric pressure. Those regions noted above that exhibit seasonal maxima in eruption rate which correspond to falling regional sea level, also exhibit seasonal maxima in eruption rate which precedes, by no more than a few months, times of independently estimated maxima in regional crustal elevation. In SW South America and at Semeru, sea level changes have relatively strong semiannual components or exhibit little regional coherence. Instead, enhanced rates of eruptions at these localities, and in Melanesia, occur during seasonal drops in atmospheric pressure.

4. Discussion

[26] In the time series shown in Figures 3–6 the variability between successive months amounts to as much as twice the standard deviation of the average monthly eruption rates. This temporal pattern in relative variability is associated with greater occurrence of eruptions worldwide in boreal winter months. On the global scale, the null hypothesis of uniform occurrence in time is rejected at the 5% significance level using the well-known Rayleigh test and as summarized in Table 5. For sufficiently long records, seasonality in worldwide eruption rate seems to be independent of the time interval considered.

[27] Key contributors to the seasonal pattern include volcanic provinces of the Pacific "Ring of Fire", including Central and South America, Kamchatka, and selected islands of Japan, and Melanesia. On local scales, even some individual volcanoes in these provinces for which detailed histories are known consistently exhibit seasonal peak levels in eruption activity. In each of these cases, individually considered, the null hypothesis of uniform occurrence of eruptions in time can be rejected at the 5% significance level using the Rayleigh test.

[28] Also indicated in Figures 3–6 are inferred global fluctuations and directly observed regional fluctuations in sea level. Seasonal cycles in sea level measured at coastal tide gauges reflect changes in air pressure, steric density, and regional runoff [*Chen et al.*, 1998; *Cazenave et al.*, 1999]. In some locations the resulting, annual change in sea level is comparable to the daily tide range. Unlike diurnal tides, however, climate-driven fluctuations in sea level correspond to changes in regional load on the marginal crust of continents and islands which are small, but which

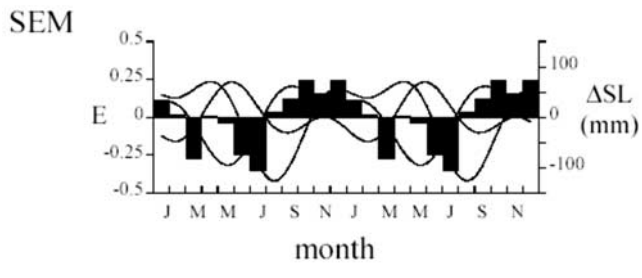

Figure 6. Monthly anomalies of volcanic eruption rate at Semuru (Java, Indonesia) during years 1997–2000. Otherwise as in Figure 2. Note that the horizontal axes span 24 months to aid in the visualization of annual patterns.

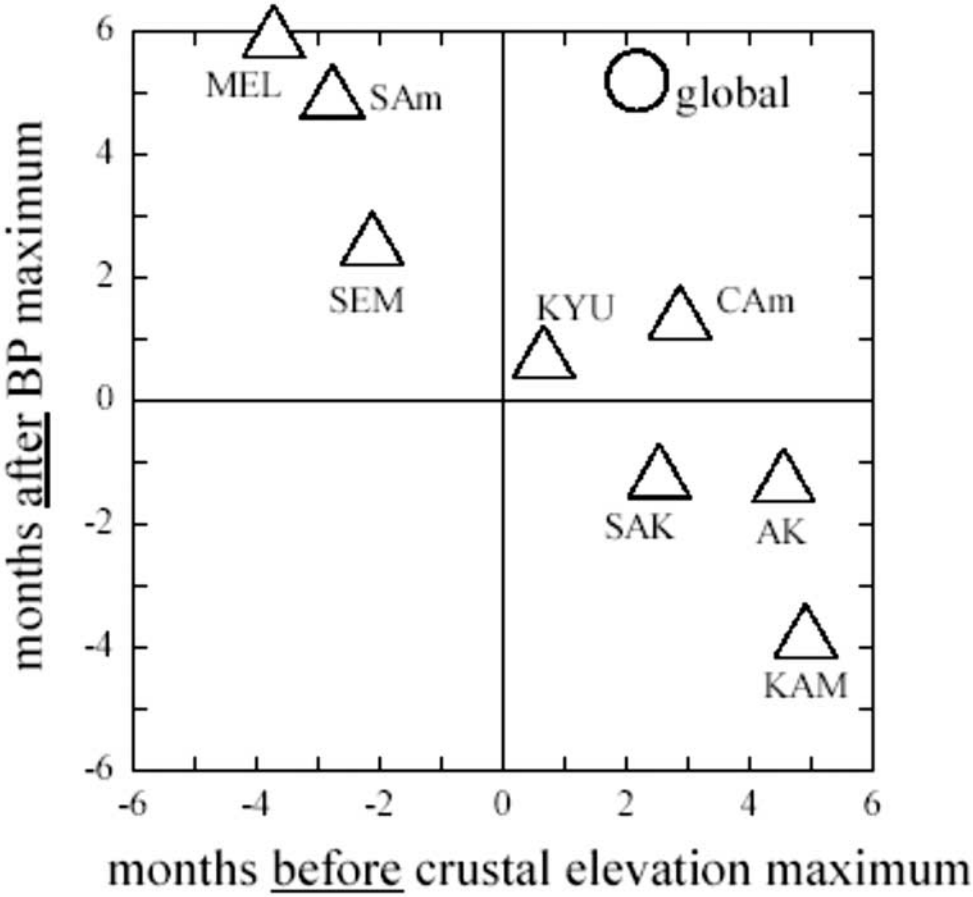

Figure 7. Phase plot indicating the timing of peak eruption rate with respect to dates of maximal values of regional crustal elevation and atmospheric pressure. Horizontal axis represents the number of months that seasonal peak in eruption activity precedes the seasonal maximum in crustal elevation associated with changes in soil moisture and snowpack (see Table 3). Vertical axis represents the number of months that seasonal peak in eruption activity follows the seasonal maximum in atmospheric pressure (see Table 4). SAm, South America; CAm, Central America; AK, Alaskan Peninsula; KAM, Kamchatka; KYU, Kyushu and Ryuku; MEL, Melanesia; SAK, Sakuru-jima; SEM, Semeru.

are nevertheless sustained for several months, act over long crustal wavelengths, and can lead to relatively long-lived changes in solid Earth surface elevation with amplitudes of up to 5–8 mm [*Chen et al.*, 1998; *Cazenave et al.*, 1999; *Mangiarotti et al.*, 2001].

[29] The links between regional seasonal eruption patterns and the seasonal changes in atmospheric pressure and crustal elevation are summarized in Figure 7. The annual changes in crustal elevation considered here are associated with changes in crustal loads due directly to snowpack thickness or soil moisture. Such changes are nominally independent of regional barometric pressure. Key observations from Figure 7 are as follows: (1) Peak eruption rates worldwide occur during intervals of global falling sea level (or rising crust) and falling atmospheric pressure averaged over subpolar latitudes. (2) Peak eruption rates along the far northern Pacific rim occur during boreal summer months, which are intervals of crustal unloading associated with melting snowpack. These are also periods of lower sea level, reflecting the local pattern of peak sea level in Autumn as a result of local meteorological factors [*Tsimplis and Woodworth*, 1994]. In this regard, recall that *McNutt and Beavan* [1987] associated the November peak of eruption occurrences at Pavlof with rising sea level. (3) Peak eruption rates at volcanoes in northern, low-latitude regions, including locales in the eastern and western Pacific basin, are associated with intervals of crustal unloading coincident with falling atmospheric pressure and crustal rising in response to loss of soil moisture. (4) Peak eruption rates at low-latitude volcanoes in the southern hemisphere, including explosive eruptions in the Andes and Melanesia and the sustained eruption sequence at the Indonesian volcano Semeru, occur 2–4 months following maximal crustal elevations but during intervals of falling atmospheric pressure. Note from Figure 4 that neither Indonesia nor SW South America is subjected to regionally consistent patterns of sea level change as measured by coastal tide gauges. Recall, however, that Melanesia exhibits a seasonal peak in eruption rate, which coincides with an annual maximum in sea level. There is thus no universally consistent pattern of correlation to annual hydrologic and climatic phenomena other than to note the following: (5) No regions exhibit

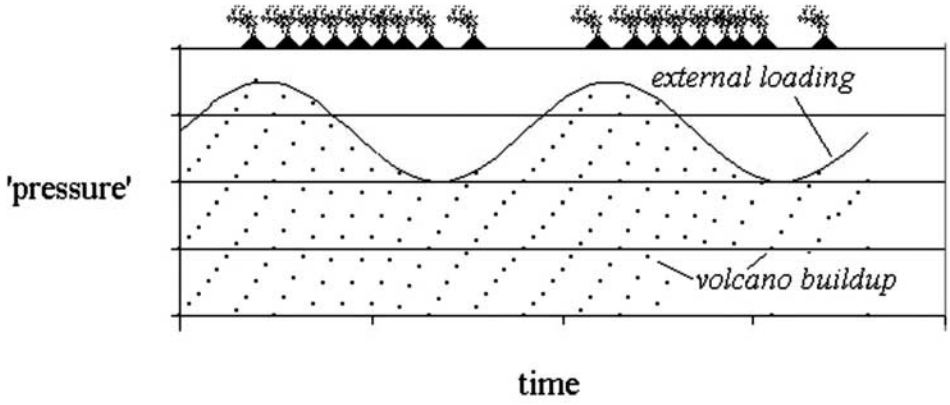

Figure 8. Schematic diagram to show how eruptions could cluster in time as the result of evolving, external loads. A series of volcanic systems (indicated by trails of dots) start off at a ''pressure'' below the threshold at which the system will erupt. Each volcanic system approaches the threshold at more or less the same rate, owing to magma buildup. The rate of approach to threshold conditions may be influenced by temporal changes in external loads and, in particular, by the mechanisms discussed in the main text. In the interpretation shown here the relationship between rates of change of magma pressure and confining external load lead to enhanced numbers of eruptions during intervals of diminishing external load. This pattern is consistent with the historical behavior of volcanoes overall, but other regional-specific relationships could apply locally owing to volcano geometry and crustal properties. A statistical description of this model and the consequent clustering of eruptions is presented by *Jupp et al.* [2004].

significant seasonal peaks in eruption rate during intervals of rising sea level and rising atmospheric pressure. This is indicated by an absence of points in the lower left quadrant of Figure 7.

[30] Having demonstrated that both global and regional patterns of volcanic seasonality exist, the logical next step is to consider what it is that is forcing this seasonal pattern of activity? If there is a single, underlying process behind the eruption seasonality, then it is not necessarily the case that the mechanism needs only to act at shallow levels in the crust (e.g., in areas susceptible to infiltration of rainwater; or susceptible to passing pressure anomalies), although such models have been proposed to explain, for example, associations between storms and small explosions at Mt St Helens [e.g., *Mastin*, 1994]. For example, in crustal rocks with an elastic modulus of order 10^{11} Pa, annual millimeter-scale deformations of, say, the uppermost 10 km of the Earth's crust, would give rise to crustal strain rates of the order of 10^{-15} s^{-1}. Such values are comparable to geological strain rates in deforming continental crust associated with other, better understood processes such as basin subsidence [*Turcotte and Schubert*, 1982], or continental plate deformation [e.g., *Shen-Tu et al.*, 1999]. Importantly, such long-period changes in crustal stress, unlike those associated with diurnal Earth tides, would elicit creep in regions of the Earth's crust and mantle with viscosities of order 10^{18} Pa s and Maxwell relaxation times of order 10^{6}–10^{7} s [*Kohlstedt and Zimmerman*, 1996; *Vigneresse et al.*, 1996], and could therefore influence partially molten regions within the Earth's crust.

[31] However, at this point, we do not consider that there is a single physical mechanism that can be thought of as ''driving'' or ''triggering'' eruptions. Instead, we suggest that a more profitable way to think about the process is that there are a host of periodic processes, which are ultimately forced by the seasonal stress imposed by the hydrological cycle. We propose that the fluctuating conditions associated with the annual movement of water mass at the Earth's surface effectively imposes a moving boundary condition on an otherwise randomly distributed [in the time sense] set of volcanic systems. This naturally results in statistically enhanced volcanic activity during annually recurring intervals of falling global sea level and atmospheric pressure. This idea is illustrated schematically in Figure 8. We have developed a full statistical model to explain this clustering of activity, which we have presented elsewhere [*Jupp et al.*, 2004].

[32] Regions that do not exhibit obvious seasonal patterns in eruption rate include the Mediterranean (although evidence for seasonality has been reported from Etna alone [*Casetti et al.*, 1981]), and some oceanic islands. While a lack of annual pattern may simply be due to incompleteness of records, it may also reflect the lack of a dominant annual phase in the crustal deformation or meteorological forcing in these locations. The absence of a seasonal signal at ocean islands (e.g., Hawaii) that we have noted here is consistent with the asymmetry in the annual variations of sea level determined by *Blewitt and Clarke* [2003]. They report seasonal peak variations in sea level ranging from 3 mm to 19 mm, with the smallest variations in the northern midlatitude Pacific, and the largest variations in polar regions. Geographical asymmetry, in terms of peak amplitude, is due to the competing effects of gravitational attraction due to land water mass that tends to draw sea level higher (this is at a peak in the Northern Hemisphere in winter) with the seasonal reduction in sea level. In the Arctic, for example, sea level peaks at 9 mm in March, while in the Antarctic, where the winter land water mass is considerably smaller, sea level peaks at 18 mm in mid-August.

[33] In summary, the recognition of seasonality in eruption rates lends qualitative support to existing ideas regarding enhanced volcanic activity during periods of global sea level change in the geologic past. If eruptive activity does indeed increase during periods of global cooling, in which ice volume increases and sea level falls, then the resulting enhanced rates of volcanogenic aerosol injection into the atmosphere may further accelerate cooling processes [cf. *Rampino et al.*, 1979; *Rampino and Self*, 1994], constituting an important feedback between global climate and volcanic activity.

[34] On shorter timescales, seasonality in eruption rate may interact with the temporal variability in the structure and circulation of the atmosphere. The altitude of the extratropical tropopause varies seasonally, and, in the Northern Hemisphere, is at a minimum during winter months [e.g., *Wong and Wang*, 2000]. Thus proportionately more northern hemisphere eruptions will inject material into the stratosphere during boreal winter [e.g., *Halmer and Schmincke*, 2003; *Mather et al.*, 2003], potentially resulting in reduced insolation and additional surface cooling. Material transport from the stratosphere to the troposphere is also seasonal, reaching a maximum in local spring [e.g., *Holton et al.*, 1995]. Seasonality in eruption rates will further amplify these effects, and may play an important role in determining the sensitivity of the climate system to those eruptions that may have widespread climatic and environmental impacts.

[35] This is but one example to illustrate that the links, and potential for feedback, between volcanic processes and the climate system may act over a range of timescales and may be both more significant and more sensitive than previously thought. If the seasonality of volcanic eruptions is indeed associated with subtle environmental changes during the annual hydrologic cycle, then active volcanic systems must be very near the critical state required for eruption. That this should be so for active volcanoes is perhaps not surprising, but nevertheless suggests further reflection upon the human capacity to alter the environment on a global scale.

5. Conclusion

[36] Volcanic activity in the last three hundred years exhibits seasonality to a statistically significant degree. This temporal pattern is observed globally; regionally along the Pacific ''Ring of Fire'' and locally at some individual volcanoes. Seasonality in eruptions is correlated with environmental fluctuations associated with the deformation of the Earth in response to the annual hydrological cycle, including falls in sea level, millimeter-scale motion of the Earth's crust, and falls in regional atmospheric pressure. The resolution of seasonal triggers of eruptions in some regions and the reasons for nonseasonality of eruptions in other regions are important challenges for the continued study of volcanoes and the mitigation of volcanic hazards.

[37] **Acknowledgments.** L. Siebert generously provided the Smithsonian eruption catalogue in digital form. Prof. Ishihara and the Volcanological Survey of Indonesia provided data from Sakura-jima and Semeru. S. Mangiorotti provided the summary of crustal motion harmonics given in Table 3. We thank C. Oppenheimer, S. Sparks, D. Nowell and T. Mather for helpful discussion and encouragement, and several anonymous individuals for critical reviews of earlier versions of the text. We thank L. Mastin, M. Jull and S. McNutt for their thorough and perceptive reviews. This work was supported by the Natural Environmental Research Council, UK (BGM, WBD), and the Newton Trust (TJ). This work formed a part of BGM's final year dissertation at the University of Cambridge.

References

Blewitt, G., and P. Clarke (2003), Inversion of Earth's changing shape to weigh sea level in static equilibrium with surface mass distribution, *J. Geophys. Res.*, *108*(B6), 2311, doi:10.1029/2002JB002290.

Blewitt, G., D. Lavallée, P. Clarke, and K. Nurutdinov (2001), A new global mode of Earth deformation: Seasonal cycle detected, *Science*, *294*, 2342–2345.

Bouillé, F., A. Cazenave, J. M. Lemoine, and J. F. Crétaux (2000), Geocentre motion from the DORIS space system and laser data to the Lageos satellites: Comparison with surface loading data, *Geophys. J. Int.*, *143*, 71–82.

Casetti, G., G. Frazzetta, and R. Romano (1981), A statistical analysis in time of the eruptive events of Mount Etna (Italy) from 1323 to 1980, *Bull. Volcanol.*, *44*, 283–294.

Cazenave, A., F. Mercier, F. Bouille, and J. M. Lemoine (1999), Global-scale interactions between the solid Earth and its fluid envelopes at the seasonal time scale, *Earth Planet Sci. Lett.*, *171*, 549–559.

Chen, J. L., C. R. Wilson, D. P. Chambers, R. S. Nerem, and B. D. Tapley (1998), Seasonal global water mass budget and mean sea level variations, *Geophys. Res. Lett.*, *25*, 3555–3558.

Cheng, M. K., and B. D. Tapley (1999), Seasonal variations in low degree zonal harmonics of the Earth's gravity field from satellite laser ranging observations, *J. Geophys. Res.*, *104*, 2667–2681.

Conover, W. J. (1980), *Practical Nonparametric Statistics*, 2nd ed., 493 pp., John Wiley, Hoboken, N. J.

Dzurisin, D. (1980), Influence of fortnightly Earth tides at Kilauea volcano, Hawaii, *Geophys. Res. Lett.*, *7*, 925–928.

Emter, D. (1997), Tidal triggering of earthquakes and volcanic events, in *Tidal Phenomena*, *Lect. Notes Earth Sci.*, vol. 66, edited by H. Wilhelm et al., pp. 293–309, Springer-Verlag, New York.

Fisher, N. I. (1993), *Statistical Analysis of Circular Data*, 277 pp., Cambridge Univ. Press, New York.

Glazner, A. F., C. R. Manley, J. S. Marron, and S. Rojstaczer (1999), Fire or ice: Anticorrelation of volcanism and glaciation in California over the past 800,000 years, *Geophys. Res. Lett.*, *26*, 1759–1792.

Halmer, M. M., and H-U. Schmincke (2003), The impact of moderate-scale explosive eruptions on stratospheric gas injections, *Bull. Volcanol.*, *65*, 433–440.

Hamilton, W. L. (1973), Tidal cycles of volcanic eruptions: fortnightly to 19 yearly periods, *J. Geophys. Res.*, *78*, 3363–3375.

Holton, J. R., P. H. Haynes, M. E. McIntyre, A. R. Douglass, R. B. Rood, and L. Pfister (1995), Stratosphere-troposphere exchange, *Rev. Geophys.*, *33*, 403–439.

Jull, M., and D. McKenzie (1996), The effect of deglaciation on mantle melting beneath Iceland, *J. Geophys. Res.*, *101*, 21,815–21,828.

Jupp, T., D. M. Pyle, B. G. Mason, and W. B. Dade (2004), A statistical model for the timing of earthquakes and volcanic eruptions influenced by periodic processes, *J. Geophys. Res.*, *109*, B02206, doi:10.1029/2003JB002584.

Kohlstedt, D. L., and M. E. Zimmerman (1996), Rheology of partially molten rocks, *Ann. Rev. Earth Planet Sci.*, *24*, 41–62.

Landsberg, H. E. (1984), *World Survey of Climatology*, 15 vols., Elsevier Sci., New York.

Mangiarotti, S., A. Cazenave, L. Soudarain, and J. F. Cretaux (2001), Annual vertical motions predicted from surface mass redistribution and observed by space geodesy, *J. Geophys. Res.*, *106*, 4277–4291.

Mastin, L. G. (1994), Explosive tephra emissions at Mount St Helens, 1989–1991: The violent escape of magmatic gas following storms?, *Geol. Soc. Am. Bull.*, *106*, 175–185.

Mather, T. A., D. M. Pyle and C. Oppenheimer (2003), Tropospheric volcanic aerosol, in *Volcanism and the Earth's Atmosphere*, *Geophys. Monogr. Ser.*, vol. 139, edited by A. Robock and C. Oppenheimer, pp. 189–212, AGU, Washington, D. C.

Matthews, A. J., J. Barclay, S. Carn, G. Thompson, and J. Alexander (2002), Rainfall-induced volcanic activity on Montserrat, *Geophys. Res. Lett.*, *29*(13), 1644, doi:10.1029/2002GL014863.

Mauk, F. J., and M. J. S. Johnston (1973), On the triggering of volcanic eruptions by Earth tides, *J. Geophys. Res.*, *78*, 3356–3362.

McGuire, W. J., R. J. Howarth, C. R. Firth, A. R. Solow, A. D. Pullen, S. J. Saunders, I. S. Stewart, and C. VitaFinzi (1997), Correlation between rate of sea-level change and frequency of explosive volcanism in the Mediterranean, *Nature*, *389*, 473–476.

McNutt, S. R. (1999), Eruptions of Pavlof volcano, Alaska, and their possible modulation by ocean load and tectonic stresses: Re-evaluation

of the hypothesis based on new data from 1984–1998, *Pure Appl. Geophys.*, *155*, 701–712.
McNutt, S. R., and R. J. Beavan (1987), Eruptions of Pavlof volcano and their possible modulation by ocean load and tectonic stresses, *J. Geophys. Res.*, *92*, 11,509–11,523.
Minster, J. F., A. Cazenave, Y. V. Serafini, F. Mercier, M. C. Gennero, and P. Rogel (1999), Annual cycle in mean sea level from TOPEX-POSEIDON and ERS-1: Inference on the global hydrological cycle, *Global Planet. Change*, *20*, 57–66.
Neuberg, J. (2000), External modulation of volcanic activity, *Geophys. J. Int.*, *142*, 232–240.
Newhall, C. G., and S. Self (1982), The volcanic explosivity index (VEI): An estimate of explosive magnitude for historical volcanism, *J. Geophys. Res.*, *87*, 1231–1238.
Rampino, M. R., and S. Self (1994), Climatic-volcanic feedback and the Toba eruption of ~74,000 years ago, *Quat. Res.*, *40*, 69–80.
Rampino, M. R., S. Self, and R. W. Fairbridge (1979), Can rapid climatic change cause volcanic eruptions?, *Science*, *206*, 826–829.
Rydelek, P. A., I. S. Sacks, and R. Scarpa (1992), On tidal triggering of earthquakes at Campi Flegrei, Italy, *Geophys. J. Int.*, *109*, 125–137.
Shen-Tu, B., W. E. Holt, and A. J. Haines (1999), Deformation kinematics in the western United States determined from Quaternary fault slip rates and recent geodetic data, *J. Geophys. Res.*, *104*, 28,927–28,955.
Simkin, T., and L. Siebert (1994), *Volcanoes of the World*, 2nd ed., 349 pp., Geoscience, Tucson, Ariz.
Stothers, R. B. (1989), Seasonal variations of volcanic eruption frequency, *Geophys. Res. Lett.*, *16*, 453–455.
Tsimplis, M. N., and P. L. Woodworth (1994), The global distribution of the seasonal sea level cycle calculated from coastal tide gauge data, *J. Geophys. Res.*, *99*, 16,031–16,039.
Turcotte, D. L., and G. Schubert (1982), *Geodynamics*, pp. 450., John Wiley & Sons, New York.
van Dam, T. M., J. Wahr, Y. Chao, and E. Leuliette (1997), Predictions of crustal deformation and of geoid and sea-level variability caused by oceanic and atmospheric loading, *Geophys. J. Int.*, *129*, 507–517.
van Dam, T., J. Wahr, P. C. D. Milly, A. B. Shmankin, G. Blewitt, D. Lavallée, and K. M. Larson (2001), Crustal displacements due to continental water loading, *Geophys. Res. Lett.*, *28*, 651–654.
Vigneresse, J. L., P. Barbey, and M. Cuner (1996), Rheological transitions during partial melting and crystallisation with application to felsic magma segregation and transfer, *J. Petrol.*, *37*, 1579–1600.
Wenzel, G., and T. Hartmann (1994), The harmonic development of the earth tide generating potential due to the direct effects of the planets, *Geophys. Res. Lett.*, *21*, 1991–1993.
Wong, S., and W-C. Wang (2000), Inter-hemispheric asymmetry in the seasonal variation of the zonal mean tropopause, *J. Geophys. Res.*, *105*, 26,645–26,659.
Wu, X., M. B. Heflin, E. R. Ivins, D. F. Argus, and F. H. Webb (2003), Large-scale global surface mass variations inferred from GPS measurements of load-induced deformation, *Geophys. Res. Lett.*, *30*(14), 1742, doi:10.1029/2003GL017546.

W. B. Dade, Department of Earth Sciences, Dartmouth College, Hanover, NH 03755, USA.
T. Jupp, Centre for Ecology and Hydrology, Natural Environment Research Council, Monks Wood, Huntingdon PE28 2LS, UK.
B. G. Mason and D. M. Pyle, Department of Earth Sciences, Cambridge University, Cambridge CB2 3EQ, UK. (bgm21@cam.ac.uk)